Tung-Hsun Chung, Wen-Hsuan Liao, and Shih-Yen Lin

The fabrication of nanomesas and nanometal contacts by using atomic force microscopy lithography

Tung-Hsun Chung,[1] Wen-Hsuan Liao,[2] and Shih-Yen Lin[1,2,3,a]

[1]*Research Center for Applied Sciences, Academia Sinica, Taipei 11529, Taiwan*
[2]*Institute of Optoelectronic Sciences, National Taiwan Ocean University, Keelung 20224, Taiwan*
[3]*Department of Photonics, National Chiao Tung University, Hsinchu 300, Taiwan*

The influence of preoxidation GaAs surface treatment over the atomic force microscopy-induced local anodic oxidation (LAO) is investigated in this paper. By immerging the GaAs samples into NaOH aqueous solutions, higher nano-oxides with better height distribution could be observed after LAO. The phenomenon is attributed to the hydrophilic surfaces obtained after the treatment such that higher local humidity and uniform water molecular distribution would be obtained on the GaAs surfaces, by using the higher nano-oxides with better height uniformity, nanomesas by using wet chemical etching, and nanometal contact after oxide lift-off are fabricated. © *2010 American Institute of Physics*. [doi:10.1063/1.3504654]

I. INTRODUCTION

Atomic force microscopy lithography (AFML) has become a promising tool to fabricate electronic and optoelectronic devices in nanometer scale in recent years.[1–4] Generally speaking, there are two major techniques of AFML. One is the nanomachining, where the sample surfaces are mechanically scratched by using AFM tips. In-plan-gated (IPG) transistor and single electron transistor have been fabricated by using this method.[2,3] The other technique is the local anodic oxidation (LAO), where local sample surface oxidation would take place with the AFM tips negatively biased. By using this method, the fabrication of IPG transistor has also been demonstrated.[4] In addition, after deoxidation of the dot-shape nano-oxides, nanoholes would be observed on the sample surfaces.[5] Therefore, site-controlled quantum dots (QDs) could be achieved by combining nanoholes and self-assembled QD growth.[5–7] Although AFML has been proved to be an efficient method to fabricate nanodevices, there are still two major disadvantages for this technique. For the LAO technique, the key issue in the oxidation procedure is the formation of water bridge between the AFM tip and sample surfaces, which makes ambient humidity an important factor to the nano-oxide formation.[8] In this case, the difficulty of precise control over the nano-oxide formation would be a major disadvantage for the LAO technique. The other disadvantage of AFML by using LAO technique is the lack of all required processing procedures for the fabrication of nanodevices such as mesa formation and metal separation. Among which, a major challenge is to put metal contacts on individual nanostructures. This is the main reason why electron beam lithography and laser interference lithography are still the major techniques adopted for the fabrication of nanodevices.[9,10]

In this paper, the content is separated into three parts: preoxidation treatment, alternating-current (ac) voltage oxidation, and the fabrication of nanomesas and nanocontacts.

In the first part, the influence of different surface treatment methods on the nano-oxides is investigated. In the second part, the difference between ac and direct-current (dc) voltage oxidation is investigated. And in the third part, the fabrication of nanomesas and nanocontacts is demonstrated by using the oxides as hard mask and lift-off medium, respectively.

II. EXPERIMENTS

The INNOVA AFM system (Veeco, Inc.) is used to conduct all AFM experiments in this paper. PtIr5-coated Si tips with a cantilevers spring constant of 0.2 N/m are employed for oxidation in contact mode. For the measurements of surface morphologies, Si tips are used in tapping mode. As for the conductive AFM (C-AFM) measurement, diamond-coated Si tip with 0.2 N/m spring constant is adopted. Through the whole oxidation process, the ambient humidity is kept at ~55%. To compare the effect of preoxidation surface treatment, three different treatments (a) no treatment, (b) immersion into 1.5% NaOH aqueous solution for 30 s, and (c) immersion into 3.7% HCl aqueous solution for 30 s are performed over n-type GaAs (100) substrates before LAO. In the study of the nano-oxides as the hard masks for mesa etching, the etching solution is: citric acid:H_2O_2:DI-water equals to 1:1:1. The process is carried out at room temperature.

III. RESULTS AND DISCUSSIONS

A. Preoxidation treatment

The average nano-oxide heights of the samples with (a) no preoxidation treatment, (b) NaOH treatment, and (c) HCl treatment under different tip biases are shown in Fig. 1(a). As shown in the figure, increasing nano-oxide height with increasing voltages is observed for all the three samples, which is attributed to the enhanced oxidation procedure with increasing electric field.[11,12] Compared with the untreated sample, higher nano-oxides are observed for the NaOH-
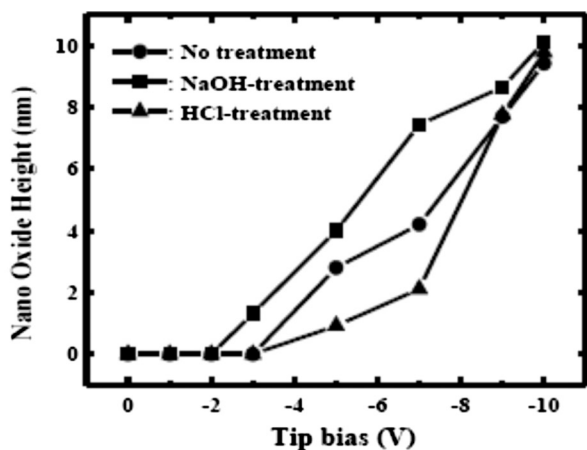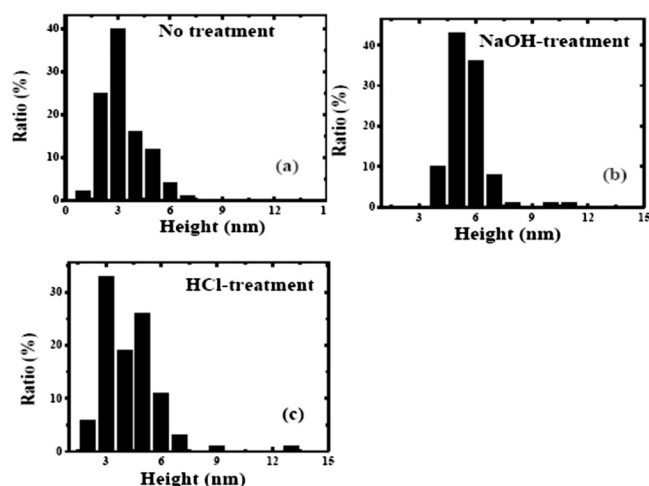
FIG. 1. (a) The average nano-oxide heights fabricated under different applied voltages from 0 to 10 V and (b) the height histograms of untreated, NaOH-treated, and HCl-treated samples.

treated sample while lower nano-oxides are observed for the HCl-treated sample. The phenomenon is attributed to the different local humidity between the AFM tips and the GaAs substrates for the three different treatments. Compared with the untreated sample, the GaAs substrates are hydrophobic after acid solution treatment and are hydrophilic after alkaline solution treatment.[13] Therefore, for the NaOH-treated sample, the local humidity near the AFM tip would be higher than the untreated sample, while lower local humidity is observed for the HCl-treated sample. In this case, the NaOH-treated sample would be of the highest nano-oxides while the HCl-treated sample would be of the lowest nano-oxides providing the sample tip bias. To investigate the height uniformity of the nano-oxides, additional three samples under the three treatment methods with 100 nano-oxides are fabricated at the applied voltage −10 V. The height histograms of the 100 nano-oxide on the three samples are shown in Fig. 1(b). As shown in the figure, compared with the other two treatments, uniform height distribution is obtained for the NaOH-

treated sample. The phenomenon is attributed to the elimination of organic molecular on the GaAs surfaces after NaOH treatment, which will enhance the size uniformity of the nano-oxides.[14] The results have indicated that NaOH treatment is advantageous for the fabrication of higher nano-oxides with better size uniformity. This pre-oxidation treatment is then performed over all the samples discussed below.
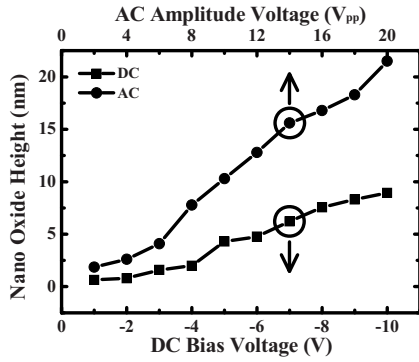
B. ac voltage oxidation

For the application in device fabrication, a high oxidation rate with better aspect ratio, defined as height/diameter, is always required. According to the tendency obtained from Fig. 1(a), one can achieve higher oxidation rate just by increasing the tip bias or slowing down the scan speed. However, with high tip biases, the coating materials on the AFM tips may be damaged. In this case, the reproducibility of the oxidation would become poor. Therefore, it has been reported elsewhere that by applying ac voltages to avoid the generation of space charge, oxidation rate would be enhanced.[15,16] In this section, the comparison of AFM LAO by using dc and ac voltages is investigated. The influence of frequencies of the ac voltages is also discussed in this section.

The AFM images of the nano-oxides obtained from dc and ac voltages are shown in Fig. 2(a), respectively. The frequency and the duty cycle for the ac voltage are 1 kHz and 70%, respectively. The average dot heights versus tip voltage are shown in Fig. 2(b). As shown in the figure, increasing oxide heights with increasing tip voltage both in ac and dc voltage are observed. Also observed are the higher oxides achieved by applying ac voltages compared with the case of dc voltages. The phenomenon suggests that it is efficient to use ac voltages to prevent the accumulation of space charges. In the dc voltage case, tip-induced oxidation in early stage will act like a capacitance, and induce space charge will accumulate to resist electrons flowing into GaAs. In this case, lower oxidation efficiency will be obtained. Hence, AFM LAO by using ac voltages would become an efficient approach to enhance the oxide height. The statistic results of aspect ratios versus tip voltages under dc and ac voltages are shown in Fig. 2(c). As shown in the figure, higher aspect ratios are also observed for the LAO by using ac voltages. This could be interpreted that the vertical oxidation rate is fast than lateral one in ac voltage, which is also resulted from reducing space charge effect.[15] The results suggest that higher oxides with higher aspect ratios would be obtained by AFM LAO applying ac voltages.

Another interesting phenomenon is the influence of ac voltage frequency on the AFM LAO. The AFM image of the nano-oxides fabricated by using different ac voltage frequencies are shown in Fig. 3(a). The scan speed, tip voltage, and duty cycle are fixed at 5 nm/s, ±8 V in ac mode, and 70%, respectively. As shown in the figure, at first, the oxide height will increase with increasing frequencies and then, decrease after the frequency higher than 100 Hz. The average heights of the nano-oxides are shown in Fig. 3(b). The phenomenon suggests that the chemical reaction responsible for the oxide formation on the GaAs surfaces does take some time to take
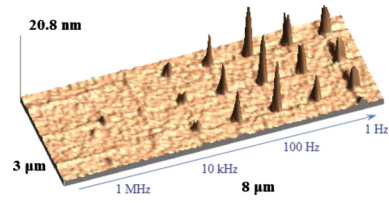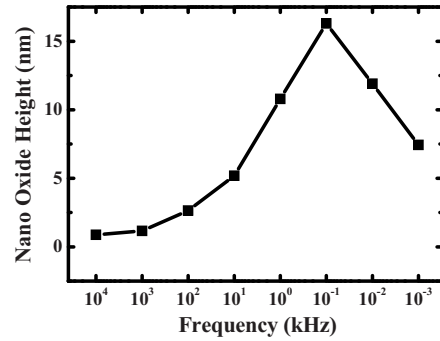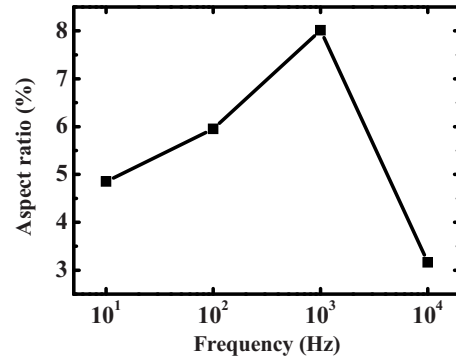
(a)

(a)

(b)

(b)

(c)
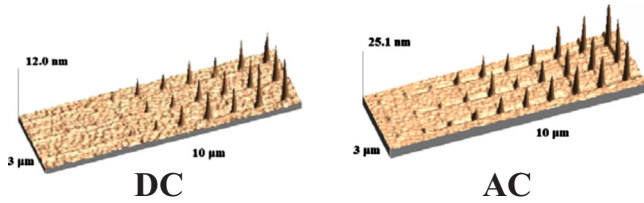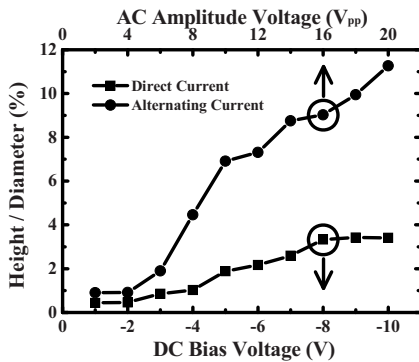
(c)

FIG. 2. (Color online) (a) The AFM images of the nano-oxides obtained from dc and ac voltages varying from 0 to 10 V, (b) the average oxide heights vs tip voltages, and (c) the aspect ratios vs tip voltages.

FIG. 3. (Color online) (a) The AFM images of the nano-oxides obtained with different ac voltage frequencies changing from 1 to 1 MHz, (b) the average oxide heights under different frequencies, and (c) the aspect ratios of the nano-oxides under different frequencies.

place.[16] Therefore, although space charge elimination by using ac voltages do help in the formation of higher nano-oxides with higher aspect ratios, reduced oxidation rate would be observed providing ac voltages with high frequencies. The average aspect ratios of the nano-oxides are shown in Fig. 3(c). As shown in the figure, although the highest nano-oxides are obtained at applied ac voltage source at 100 Hz, the highest aspect is observed at 1 kHz. Therefore, 1 kHz is chosen for the following experiments.

C. The fabrication of nanomesas and nanocontacts

The first task for the development of AFML is the fabrication of nanomesas. To achieve this goal, an etching solution with high selectivity between the nano-oxides and the GaAs substrates is required. The etching solution adopted in this paper is: citric acid : H_2O_2 : DI-water = 1 : 1 : 1. The nano-

oxides are fabricated with scan speed 3 nm/s under an ac voltage ±10.0 V on the GaAs surfaces. The nanomesas are fabricated by dipping the sample with nano-oxides into the etching solution for 3 min. The nano-oxides remained on the top of the nanomesas are removed by dipping the sample into 3.7% HCl aqueous solution. The schematic fabrication flow chart of the nanomesas and the 6×6 nano-oxides and nanomesas are shown in Figs. 4(a)–4(c), respectively. As shown in the figure, nanomesas with diameter/height 420/30 nm can be fabricated with high uniformity. Also observed in Fig. 4(c) are the sharp tips instead of flat tops on the nanomesas. The results suggest that although the etching rate of the HCl aqueous solution is higher for oxides than GaAs, the minor etching effect over GaAs would still result in sharp tips on the mesas instead of flat top after oxide removal. Following the same approach, rectangular nanomesas with
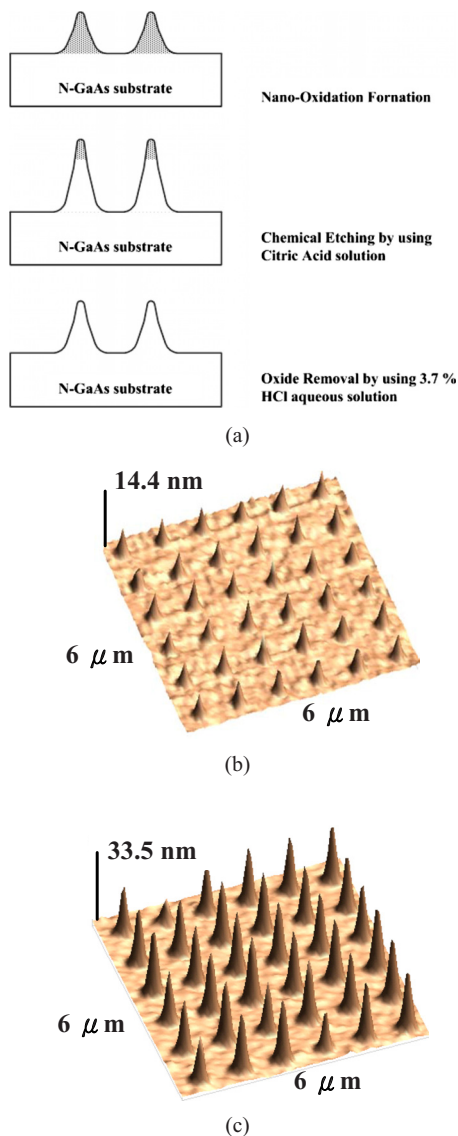
FIG. 4. (Color online) (a) The schematic fabrication flow chart of the nanomesas and the AFM images of 6×6 (b) nano-oxides and (c) nanomesas.

FIG. 5. (Color online) The AFM image of the 6×4 2-μm-long rectangular nanomesas.

rings and achieve metal separation. After oxide lift-off, the sample is thermally annealed at 350 °C for 5 min to achieve Ohmic contact. The AFM image image of the nanocontacts formed by using the oxide lift-off procedure is shown in Fig. 6(b). As shown in the figure, metal separation could be easily achieved by using this method. To investigate the actual electrical isolation of this approach, the C-AFM image of the sample is shown in Fig. 6(c). The bias across the tip and sample is −10 V, and the tip is grounded. As shown in the figure, the similar current level inside and outside the ring trench suggests that Ohmic contacts are obtained in the both regions. The low current flow in the circle trench region suggests that good electrical isolation could be achieved via the lift-off procedure of the nano-oxides. The results have demonstrated that the nano-oxides fabricated by using AFM could not only act as hard masks for mesa formation. The lift-off procedure of ring oxide after metal deposition could also be applied for he fabrication of nanocontacts. At this stage, the smallest diameter of the nano-oxides could achieve 90 nm as shown in Fig. 6(c). To further clarify the fabrication procedure of the nanocontacts, a schematic fabrication flow chart of the nanocontacts is shown in Fig. 7.

IV. CONCLUSIONS

In conclusion, the fabrication of nanomesas and nanocontacts by using nano-oxides obtained over the AFM-

width/length/height: 412/2000/41 nm can also be fabricated by using oxide lines as the hard masks. The AFM image of the rectangular nanomesas is shown in Fig. 5. As shown in the figure, well-aligned rectangular nanomesas with high uniformity could also be obtained by using nano-oxides as the hard masks. The results have demonstrated excellent one-to-one correspondence between the nano-oxide hard masks and the nanomesas by using wet chemical etching.

The other challenge for AFML is the fabrication of nanocontacts. Unlike the application of hard masks of nanooxides for the nanomesa fabrication, the nano-oxides may act as a lift-off medium to separate metal contacts. To achieve this goal, ring-shape nano-oxides with different diameters are fabricated with 30 nm/s scan speed and tip bias ac 10.0 V. The AFM image of the oxide rings are shown in Fig. 6(a). After the oxidation procedure, 4nm Au/Ge alloy followed by additional 4 nm Au are deposited on the sample. The deposition of the 4 nm Au/Ge is for the formation of Ohmic contacts. After the metal deposition, the sample is dipped into the 3.7% HCl solution for 1 min to remove the oxide
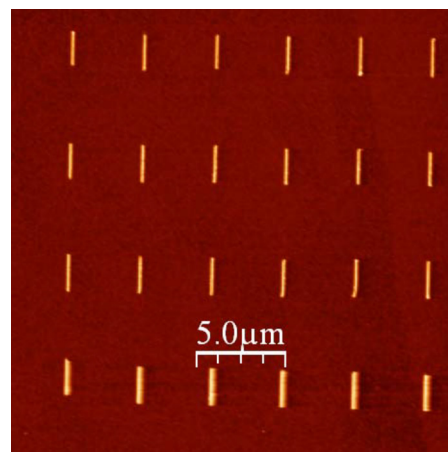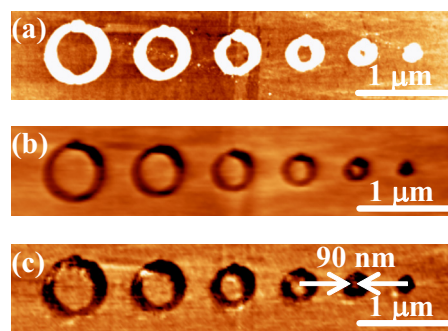

FIG. 6. (Color online) The AFM images of (a) nano-oxides and (b) nanocontacts. The C-AFM image of the nanocontacts is shown in (c). When measuring the C-AFM, the bias across the tip and sample is −10 V, and tip is grounded.
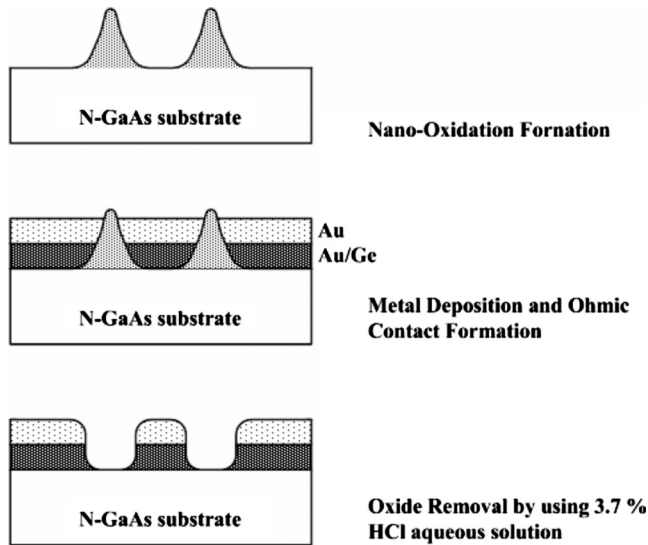
FIG. 7. The schematic fabrication flow chart of the nanocontacts.

induced LAO is investigated. By using NaOH treatment, higher oxides with better uniformity are obtained on GaAs substrates. Enhanced nano-oxide heights and aspect ratios are observed for the AFM LAO by using ac voltage source. It is demonstrated that nanomesas and nanocontacts could be fabricated by using the oxides as the hard mask and lift-off medium, respectively. The C-AFM image of the nanocontacts has demonstrated good electrical isolation of this technique. The development of AFML is quite advantageous for the next-generation nanodevice fabrication.

[1] S. C. Minne, H. T. Soh, P. Flueckiger, and C. F. Quate, Appl. Phys. Lett. **66**, 703 (1995).
[2] H. W. Schumacher, U. F. Keyser, R. J. Haug, and K. Eberl, Appl. Phys. Lett. **75**, 1107 (1999).
[3] U. F. Keyser, H. W. Schumacher, U. Zeitler, R. J. Haug, and K. Eberl, Appl. Phys. Lett. **76**, 457 (2000).
[4] R. Held, T. Vancura, T. Heinzel, K. Ensslin, M. Holland, and W. Wegscheider, Appl. Phys. Lett. **73**, 262 (1998).
[5] J. S. Kim, M. Kawabe, and N. Koguchi, J. Appl. Phys. **88**, 072107 (2006).
[6] S. Y. Lin, C. C. Tseng, T. H. Chung, W. H. Liao, S. H. Chen, and J. I. Chyi, Nanotechnology **21**, 295304 (2010).
[7] H. Z. Song, T. Usuki, T. Ohshima, Y. Sakuma, M. Kawabe, Y. Okada, K. Takemoto, T. Miyazawa, S. Hirose, Y. Nakata, M. Takatsu, and N. Yokoyama, Nanoscale Res. Lett. **1**, 160 (2006).
[8] H. Jungblut, D. Wille, and H. J. Lewerenz, Appl. Phys. Lett. **78**, 168 (2001).
[9] M. A. Reed, J. N. Randall, R. J. Aggarwal, R. J. Matyi, T. M. Moore, and A. E. Westel, Phys. Rev. Lett. **60**, 535 (1988).
[10] J. de Boor, N. Geyer, J. V. Wittemann, U. Gösele1, and V. Schmidt, Nanotechnology **21**, 095302 (2010).
[11] P. Avouris, T. Hertel, and R. Martel, Appl. Phys. Lett. **71**, 285 (1997).
[12] Y. Okada, S. Amano, M. Kawabe, and J. S. Harris, Jr., J. Appl. Phys. **83**, 7998 (1998).
[13] S. Osakabe and S. Adachi, J. Electrochem. Soc. **144**, 290 (1997).
[14] J. D. Plummer, M. D. Deal, and P. B. Griffin, *Silicon VLSI Technology Fundamentals Practice and Modeling* (Prentice Hall, New Jersey, 2000), Chap. 5.
[15] J. A. Dagata, T. Inoue, J. Itoh, K. Matsumoto, and H. Yokoyama, J. Appl. Phys. **84**, 6891 (1998).
[16] Y. Matsuzaki, S. Hasui, S.-Y. Kamada, A. Yamada, and M. Konagai, Jpn. J. Appl. Phys., Part 1 **40**, 4325 (2001).